Journal of Scientific Research and Advances

ISSN 2395-0226

TO IMPROVE THERMAL CYCLES OF QUARTZITE CONTAINING RAMMING MASSES, APPLIED IN INDUCTION FURNACE

Manjeet Kumar Shukla[1], Satyendra Kumar Singh[2] and Vinay Kumar[3]

[1] Department of Ceramic Engineering, Indian Institute Of Technology (BHU), Varanasi, Uttar Pradesh, INDIA 221005
E-mail address:manjeetkumarshukla@gmail.com
[2] Department of Ceramic Engineering, Indian Institute Of Technology (BHU), Varanasi, Uttar Pradesh, INDIA 221005
[3]Department of Ceramic Engineering, Indian Institute Of Technology (BHU), Varanasi, Uttar Pradesh, INDIA 221005

Abstract: The ramming mass is the class of monolithic refractory. Ramming masses are first mixed with water or any other liquid to the required quality, and then rammed either manually or pneumatically with a heavy rammer. There is a class of refractory material which can form joint-less lining. This class of refractory material is called monolithic. All unshaped refractory materials have this ability to form joint-less lining and hence they are grouped as monolithic. In proposed work silica ramming masses particles were coated by zirconia (ZrO_2) for densification and to improve slag resistance. The evolution of crystalline phases and the microstructures have been studied using X-ray diffractometer. Physico-mechanical properties such as bulk density, apparent porosity, cold crushing strength, and cold modulus of rupture were investigated. Slag resistance and permanent linear shrinkage were also observed. Change of bulk density and apparent porosity with ZrO_2 content has been observed. It has been found that bulk density of quartzite increases with increasing amount of ZrO_2 due to higher density of zirconia itself. Apparent porosity decreases with the addition of zirconia. The slag resistance of refractory material is measured by loss of weight per unit area per unit time or a rate of penetration, i.e. the thickness of refractory material lost. In practice it is not usually possible to eliminate all corrosion damage to refractory used for the construction of industrial application. There is significant increase in the slag resistance with increasing amount of zirconium dioxide. This behavior is due to coating of ZrO_2 on silica mixture which improves the packing density of the samples. The reason of increasing slag resistance is that zirconium dioxide form protective layer around the quartzite particle. There is significant increase in the slag resistance with increasing amount of zirconium dioxide. This leads finally to a much denser structure as when compared to sinter at lower temperature.

Keywords: ramming mass, X-ray diffractometer, modulus of rupture, bulk density, and apparent porosity, slag resistance

INTRODUCTION

The past three decades achieved a significant progress in refractories technology that resulted in a remarkable reduction in refractories consumption. 'Refractories', a key input for iron and steel making, assumed ever-increasing sophisticated steels. These materials, enabling the utilization of heat to prepare articles since long back, involve nowadays the use of stringent quality shaped and unshaped materials tailored for specific applications with improved thermo-mechanical and corrosion-resistant properties.

In the second half of the last century, basic oxygen process with larger vessel started reaching popularly to the steel makers. Many processes had been tried and a few proved very successful not only in making steel but also to produce it quicker with larger amount, putting greater demand on the refractories quality. With this, the technology of new phase of production and application of refractories entered endearingly to the picture. Simultaneously, the cost-effectiveness of refractory required per tonnage of steel became important to the manufacturers. As the improvement of quality and consistency of the refractory materials proved to be essential to help customers, for the best possible performance, at the least possible cost, under the given circumstances. The most noticeable development and application of refractories, in this regard, have been found in the field of unshaped monolithic refractories. From the retrospective inside India and abroad, a significant replacement of shaped refractory products by monolithic has been observed both in ferrous, non-ferrous, cement, glass and ceramic industries.

Evolution of monolithic refractories aimed at building up of a construction which itself is a single unit to indicate a noteworthy change from labour intensive brick manufacturing technique since 1960s. The present day scenario shows a great increase in the shaped refractory bricks. [1]

II. LITERATURE REVIEW

Today's dense ramming mass systems have complex compositions comprised of the generic materials such as aggregates, fine reactive fillers like zirconia and silica. The entire system can be considered to be an independent system and the final characteristics are as a result of the sum of interactions of all. Depending on the specific type of refractory, the aggregate and matrix may be of similar or vastly different in chemical and physical properties. It is evident that almost infinite combinations exist. When different aggregates, bonding matrices and particle size distributions for a particular type of ramming are considered. The relative proportion of the constituents, their chemistry and mineralogy influence the flow and refractory property of the ramming. A good ramming mass must not only have good purity but must also have good compactness or packing density. This property depends upon the proportion of grains of different sizes which will give least to open space between the particles. Statistically it is possible to achieve good compactness with different proportions of particles. But it may be possible that though statistically one combination may appear attractive from the point of view of compactness it may not work because sintering may be poor or mechanical strength may not be proper. Different manufacturers have standardized on different proportions they have tried and tested over the last several years. The product is used for bronze, white, and purple copper-melting. [2]

III. EXPERIMENTAL WORK

(1) Synthesis of Materials:

The materials used in present work are Quartzite (Shiva minerals Pvt. Ltd.) ZrO_2 and Boric acid (Loba Cheme Pvt.Ltd.).The quartzite was prepared as aggregate by crushing and grinding it in a planetary ball mill and then sorting it via sieves into the size of 0 to 6 mm. The specific gravity of quartzite is 2.35 g/cm^3. The batch composition of the samples are listed in Table.1

Table.1 Batch Composition

Sample	Quartzite (%)	Zirconium dioxide (%)	Boric acid
Z_0	100	0	2.5
Z_5	95	5	2.5
Z_{10}	90	10	2.5
Z_{20}	80	20	2.5

(2) Sample preparation for different experiment:

(2.1)Sample preparation for X-ray diffraction analysis:

Material was crushed and ground to fine particle. Then contaminated iron particles were removed. Then the powder was fined in agate mortar to get more fine powder to pass through 200 mesh BS sieves.

(2.2) Sample preparation for CCS:

Surface grinding of sintered bar samples were done to get parallel plane so that applied load during testing act uniformly. Then measurements of width and depth were taken of each sample.

(3)Bulk Density and Apparent Porosity Measurements: Bulk densities of the sintered pellets were determined from geometrical dimension and mass of the pellets. ASTM C914 is employed for this measurement.

$$\mathbf{B.D.} = \frac{\mathbf{D}}{(\mathbf{W}-\mathbf{S})} \boldsymbol{gm/cc}$$

The method used for the determination of apparent porosity of pellets is boiling point method. First the pellets are dried in oven at 100°C to a constant weight D with an accuracy of 0.001 gm. The dried pellet is suspended in distilled water such that the pellets do not touch bottom or sides of the container. It is boiled for 2 hours still suspended in water cooled at room temperature and its weight (S) is noted. The pellets are removed from water and extra water is wiped off from its surface by lightly blotting with the wet towel and is weighed in air (W).

The apparent porosity (A.P.) is then calculated by the follwoing formula.

$$\boldsymbol{A.P.} = \frac{\boldsymbol{W}-\boldsymbol{D}}{\boldsymbol{W}-\boldsymbol{S}} \times \mathbf{100}$$

Where W-D= actual volume of the open pores of the pellets

W-S = external volume of the specimen.

(4) Cold Crushing Strength: According to ASTM C133 the cold strength of a refractory material is an indication of its suitability for use in refractory construction. (This is not a study of performance at elevated temperatures.) These test methods are for determining the room temperature flexural strength in 3-point bending (cold modulus of rupture) or compressive strength (cold crushing strength), or both, for all refractory goods. This Considerable are must be used to compare the results of different determinations of the cold crushing strength or modulus of rupture. The sample dimension and shape, the character of the specimen faces (that is, as-formed, sawed, or ground), the orientation of those faces for the period of testing, the load geometry, and the rate of weight application, may all considerably influence the mathematical results obtained.

Comparisons of the results between different determinations should not be made if one or more of these parameters differ between the two determinations. The comparative ratio of the biggest grain size to the smallest specimen dimension may significantly affect the mathematical result. For example, lesser, cut sample containing big grains may present different results than the bricks from which they are cut. Under no situation should 6- by 1- by 1-in. (152- by 25- by 25-mm) specimens be prepared and tested for materials containing grains with a maximum grain dimension more than 0.25 in. (6.4 mm).

This test method is useful for study and improvement, engineering application and design, manufacturing process control, and for developing purchasing specifications. [3]

(5) X-ray diffraction (XRD):X-ray diffraction employs electromagnetic waves with a wavelength of the order of one angstrom. Since wave diffraction occurs when the dimensions of the diffracting object are of the same order of magnitude as the wavelength of the incident wave, x-rays are ideally suited to probe crystal lattice structures.

(6) Modulus of Rupture : Modulus of rupture (MOR) test was carried out under three-point bending tests (ASTMC133-97) using 50mm×10mm×10mm samples. Modulus of rupture was calculated using the following formulae:

$$\mathbf{MOR= (3PL)/ (2bd^2)}$$

Where, MOR=modulus of rupture (M Pa), P=maximum force applied at rupture (N), L=span between supports (mm), b=width of specimen (mm), and d=depth of specimen (mm). Modulus of rupture was calculated at room temperature using universal materials test equipment.

(7) Permanent Linear Change: According to ASTM-C113 Refractory brick and shapes of different compositions exhibit unique permanent linear changes after heating or reheating. This testing method provides a standard process for heating various types of refractories with appropriate heating schedules. Linear reheat changes obtained by this test method are appropriate for use in research and development.

(8) Corrosion resistance (Slag resistance): The property of refractory materials to defend against the action of molten slags. Slag resistance is calculated by the loss in volume or weight of a refractory material by the action of a slag and, the depth of penetration of the slag into the refractory material. Both stationary methods (dissolving of a refractory material in a set amount of slag) and dynamic methods are used to determine slag resistance; both methods may be used. Corrosion resistance depend on the chemical behaviour of the slag and the refractory material and also depend on the density and structural features of the refractory material.

Corrosion is the degradation of materials by chemical action with the environment. The corrosion is applied to the wear and tear of plastics, concrete and wood but normally refers to metals. [4]

IV. RESULTS AND DISCUSSION:

(1) Bulk density (BD) and apparent porosity (AP) Measurement:

BD and AP were determined at temperatures (1600°C). Figure 1. shows that in $\mathbf{Z_0}$, $\mathbf{Z_5}$, $\mathbf{Z_{10}}$ and $\mathbf{Z_{20}}$ there is significant increment in the densification accompanied by valuable decrement in the porosity in correlation with increasing amount of ZrO_2. In the temperature series 110 °C to 1100 °C this behaviour is due to the fine particle size distribution of the silica mixture which improves the packing density of the samples. This leads finally to a much denser structure as when compared to sintered at lower temperature.

Table 2. Apparent porosity and bulk density of sample

SAMPLE	APPARENT POROSITY (%)	BULK DENSITY (gm/cc)
Z_0	19.5	2.29
Z_5	18.2	2.37
Z_{10}	17.4	2.48
Z_{20}	16	2.54

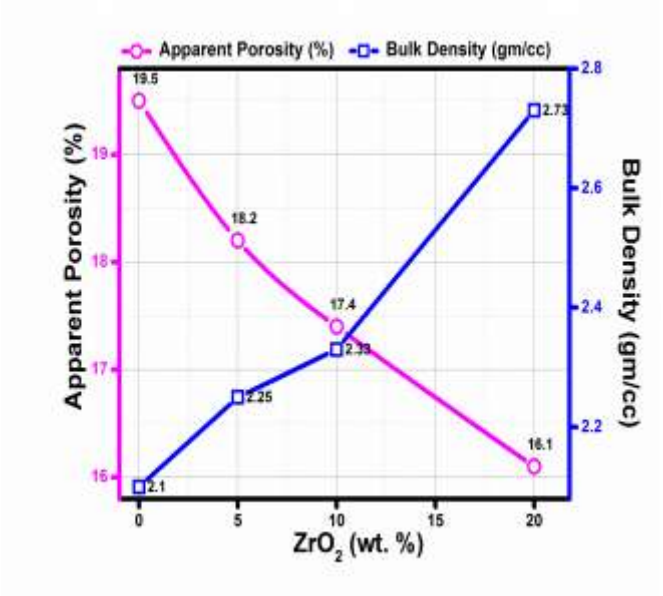

Figure 1. Bulk density (BD) and apparent porosity (AP) measurement

Discussion: BD and AP of all the samples as a function of zirconium dioxide. Bulk density has increasing trend with zirconium dioxide (ZrO_2) content. Apparent Porosity has decreasing trend with zirconium dioxide (ZrO_2) content shown in figure 1.

Densification:

The role of densification is very important in ceramic fabrication process. Densification is the process which is achieved by sintering at high temperature. It is mainly done by diffusion process. Ceramic bonds are responsible for fired strength. The diffusion process is affected by some minor addition (additive).Because of this additive densification and degree of densification changes. Densification is shown in terms of bulk density (BD) and apparent porosity (AP).

On sintering, quartzite without additive shows high apparent porosity. This higher amount of apparent porosity is due to formation of liquid phase that also observed in X-ray diffraction analysis. Additives were used to arrest the formation of this liquid phase which degrades the refractory properties.

Effect of ZrO_2 on densification:

Change of bulk density and apparent porosity with ZrO_2 content has been shown in Figure1. It has been found that bulk density of quartzite increases with increasing amount of ZrO_2 due to higher density of zirconia itself. Apparent porosity decreases with the addition of zirconia.

(2) Cold crushing strength (CCS) Measurement:

CCS of all the samples as a function of zirconium dioxide are shown in Figure 2. It can be observed from Figure 2. That at $\mathbf{Z_{20}}$ sample containing 20 wt% zirconium dioxide and 80% quartzite depicts the highest strength.$\mathbf{Z_0}$ sample has low CCS value.

Table 3. CCS of samples

Sample	Cold crushing strength (M pa)
Z_0	205
Z_5	219
Z_{10}	256
Z_{20}	278

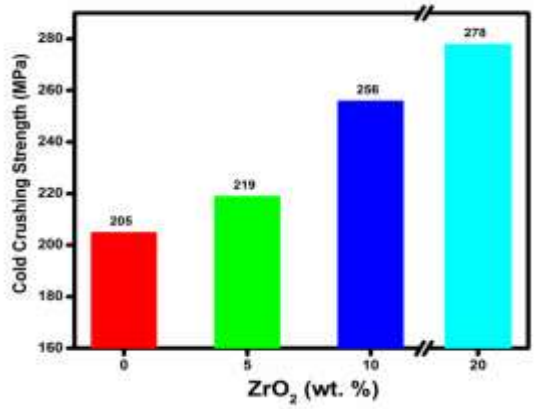

Figure 2. Cold Crushing Strength vs. ZrO_2 (wt. %)

Discussion: The variation of cold crushing strength (CCS) of the samples sintered at 1600ºC for 2h is shown in Figure 2. Cold crushing strength (CCS) of all the samples as a function of zirconium dioxide. The CCS value shows an increasing trend with increasing amount of ZrO_2. This trend is due to the toughening nature of ZrO_2 present at grain boundaries. And also lower amount of liquid formation as well as change of grain morphology of quartzite grains to sub rounded shape is responsible for this increasing trend, which is evident from the microstructure also.

(3) Structure & Phase Identification by X-ray diffraction:

Evolution of the phases by X-Ray diffraction shown in Figure 3. is the XRD patterns of samples fired at 1500^0C $\mathbf{Z_0}$, $\mathbf{Z_5}$, $\mathbf{Z_{10}}$ and $\mathbf{Z_{20}}$. The major phase quartzite formation in all samples is indicated at 1500^0C.

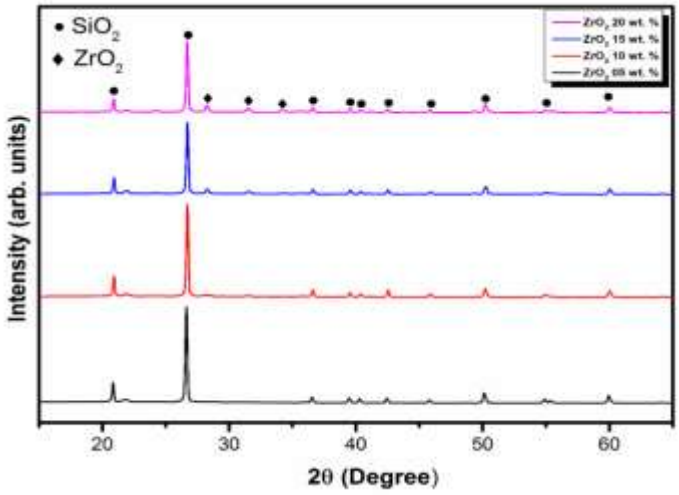

Figure 3. X-Ray Diffraction plot of prepared SiO_2-ZrO_2

Discussion: There is no new phase formation after firing. The zirconium dioxide (ZrO_2) provides a protective layer for quartzite particle.

4. Modulus of Rupture (MOR) Measurement:

Modulus of rupture of the fired samples were calculated as zirconia contain is increasing the density is increasing and modulus of rupture gets varied from 17MPa to 24MPa.

Table 4. MOR of Samples

Sample	Modulus of rupture (M pa)
$\mathbf{Z_0}$	17
$\mathbf{Z_5}$	20
$\mathbf{Z_{10}}$	24
$\mathbf{Z_{20}}$	21.5

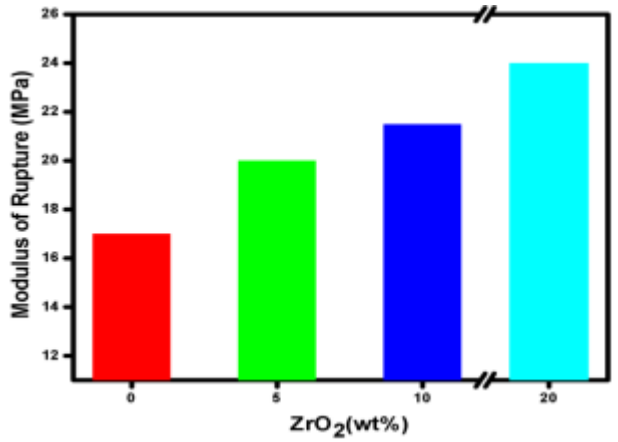

Figure 4. Modulus of Rupture vs. ZrO_2 (wt. %)

Discussion: The variation of Modulus of rupture (MOR) of the samples sintered at 1600ºC for 2h is shown in Figure 4.The MOR value shows an increasing trend with increasing amount of ZrO_2 but MOR value is highest for 20% ZrO_2 content. This trend is due to the toughening nature of ZrO_2 present at grain boundaries. And also lower amount of liquid formation as well as change of grain morphology of quartzite grains to sub rounded shape is responsible for this increasing trend, which is evident from the microstructure also.

(5) Permanent Linear Change (PLC) Measurement:

Table 5. PLC of Samples

Sample	PLC (%)
Z_0	2.9
Z_5	2.4
Z_{10}	1.9
Z_{20}	0.4

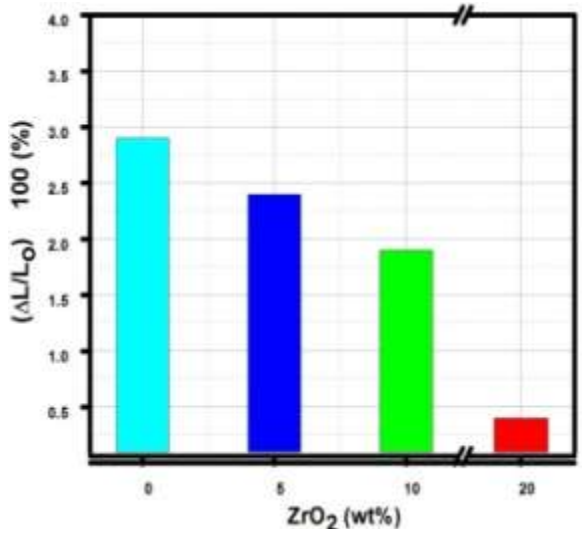

Figure 5. Permanent Linear Change vs. ZrO_2 (wt. %)

Discussion: Permanent Linear Change (PLC) of all the samples as a function of zirconium dioxide. The PLC value shows a decreasing trend with increasing amount of ZrO_2 shown in figure 5.

(6) Corrosion resistance (Slag resistance):

The slag resistance of refractory material is measured by loss of weight per unit area per unit time or a rate of penetration, i.e. the thickness of refractory material lost. In practically it is not usually possible to eliminate all corrosion damage to refractory used for the construction of industrial application. The rate at which slag attack on refractory is usually expressed in one of two ways:

(1) Loss of weight per unit area per unit time.

(2) A rate of penetration, i.e. the thickness of refractory material lost.

Slag resistance were determined for all the samples $\mathbf{Z_0}$,$\mathbf{Z_5}$, $\mathbf{Z_{10}}$ andZ_{20} fired at temperature (1500°C). Figure shows that in $\mathbf{Z_0}$,$\mathbf{Z_5}$, $\mathbf{Z_{10}}$ and $\mathbf{Z_{20}}$ there is significant increase in the slag resistance with increasing amount of zirconium dioxide. This behaviour is due to the fine particle size distribution of the silica mixture which improves the packing density of the samples. At 1600 °C reactions between silica and zirconium dioxide forms a phase filling the inter-spaces among the constituents of samples. This leads finally to a much denser structure as when compared to sintered at lower temperature.

6.1 Effect of ZrO_2 on slag resistance:

The variation of slag resistance (corrosion resistance) of the samples sintered at 1600ºC for 2h is shown in Fig. The slag resistance shows an increasing trend with increasing amount of ZrO_2. This trend is due to the toughening nature of ZrO_2 present at grain boundaries. And also lower amount of liquid formation as well as change of grain morphology of quartzite grains to sub rounded shape is responsible for this increasing trend, which is evident from the microstructure also.

The reason of increasing slag resistance is that zirconium dioxide form protective layer around the quartzite particle. Figure shows that in $\mathbf{Z_0}$,$\mathbf{Z_5}$, $\mathbf{Z_{10}}$ and $\mathbf{Z_{20}}$ there is significant increase in the slag resistance with increasing amount of zirconium dioxide composition of slag is given in table 1.

Table 6. Composition of Slag

Components	% of Components
Fe_2O_3	22
SiO_2	27.5
Al_2O_3	15
MnO	3.0
MgO	8.0
CaO	22
TiO_2	2.0
V_2O_5	0.5
C/S	0.8

Figure 6. pellets of slag

Figure 7. Sample with pellets of slag

Figure 8. Sample after penetration of slag

Discussion: The longitudinal section of the test sample cut at the midpoint as shown in figure. Figure indicates that the corrosion resistance of the sample increase with an increase in ZrO_2 content in the sample. The experimental result shows that the slag resistance of sample mainly depends on ZrO_2 content, temperature etc.

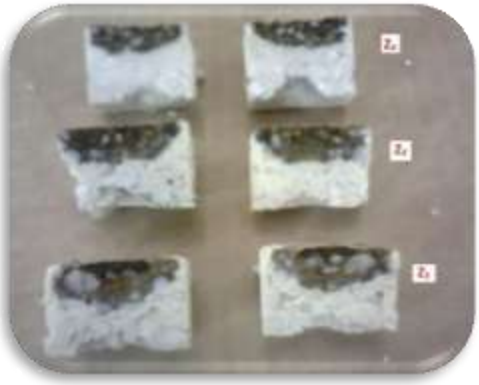

Figure 9. Slag penetration in sample
Z_1 = 0% ZrO_2
Z_2 = 5% ZrO_2
Z_4 = 20% ZrO_2

6.2 Effect of temperature on penetration:

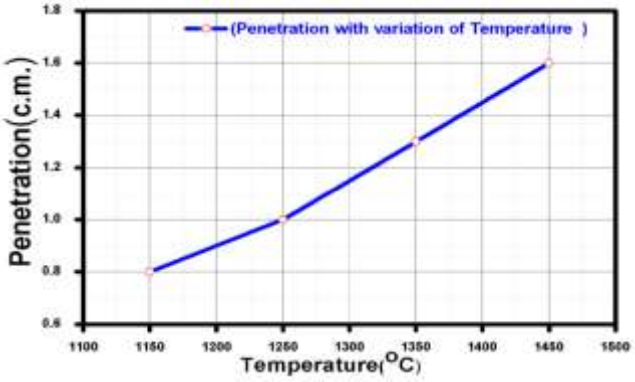

Figure 10. Penetration vs. Temperature

Discussion: Graph indicates that the penetration of the slag in test sample increases with an increase in temperature. The slag resistance shows a decreasing trend with increasing temperature. This trend is due to the amount of liquid formation as well as change of grain morphology of quartzite grains, which is evident from the microstructure also.

6.3 Effect of time on penetration:

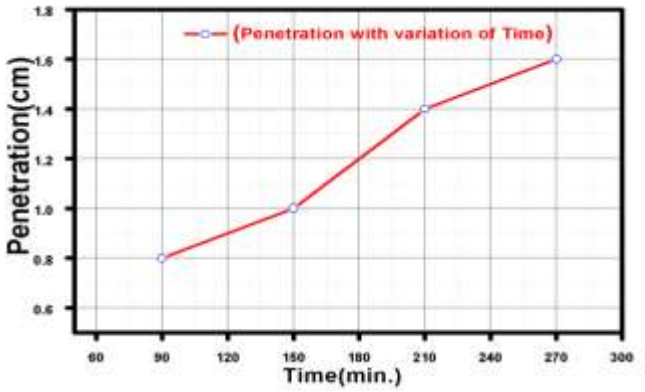

Figure 11. Penetration vs. Time (min.)

Discussion: Graph shown in figure 11. Indicates that the penetration of the slag in test sample increases with an increase in penetration time. The slag resistance shows a decreasing trend with increasing penetration time. With increasing penetration time, the slag more penetrates in to the sample.

6.4 Effect of ZrO_2 (wt %) on penetration:

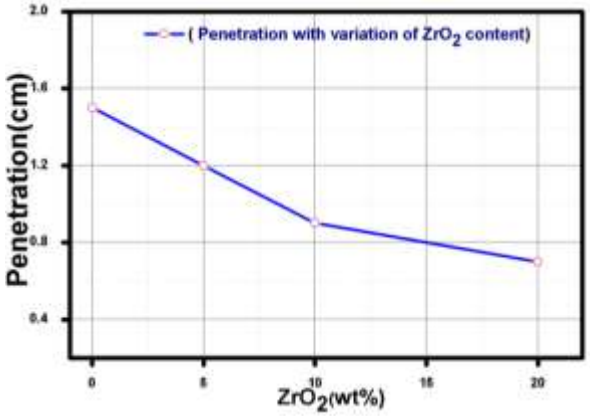

Figure 12. Penetration vs. ZrO_2 (wt %)

Discussion: The reason of increasing slag resistance is that zirconium dioxide form protective layer around the quartzite particle. Figure 12. Shows that in **Z_0**, **Z_5**, **Z_{10}** and **Z_{20}** there is significant increase in the slag resistance with increasing amount of zirconium dioxide. The role ZrO_2 composition in the slag resistance of quartzite ramming masses is to dissolve itself in the penetrating slag and as a result to decrease the penetration. The slag resistance shows an increasing trend with increasing amount of ZrO_2. This trend is due to the toughening nature of ZrO_2 present at grain boundaries. And also lower amount of liquid formation as well as change of grain morphology of quartzite grains to sub rounded shape is responsible for this increasing trend, which is evident from the microstructure also.

V. Conclusion:

In the present investigation the various characteristics of silica ramming mass were studied and the sintering temperature was optimized. Zirconia (ZrO_2) was incrementally added to formulate dense silica ramming masses. Various characteristics like PLC, AP, BD, CCS, MOR& slag resistance analysis were performed. Zirconium oxide increase slag resistance of silica ramming masss.The reason of increasing slag resistance is that zirconium dioxide form protective layer around the quartzite particle

REFERENCES

[1]. Shenyang Jiyongli Refractory Materials Co., Ltd.

[2]. Yung-Chao Ko, Role of spinel composition in the slag resistance of Al_2O_3–spinel and Al_2O_3–MgO castables, Ceramics International 28 (2002)

[3]. Kyong Yun Yeau, Eun Kyum Kim, An experimental study on corrosion resistance of concrete with ground granulate blast-furnace slag, Cement and Concrete Research 35 (2005)

[4]. Mun-Kyu Cho, Gi-Gon Hong, Seok-Keun Lee, Corrosion of spinel clinker by CaO–Al2O3–SiO2 ladle slag, Journal of the European Ceramic Society 22 (2002)

[5]. S. Mukhopadhyay, T.K. Pal, P.K. DasPoddar, Improvement of corrosion resistance of spinel-bonded castables to converter slag, Ceramics International 35 (2009)

[6]. ASTM C133 Crush Modulus Rupture Refractories Test Equipment

[7]. R.K. Pati, P. Pramanik, Low temperature chemical synthesis of nanocrystalline MgAl2O4 spinel powder, J. Am. Ceram. Soc. 83 (2000) 1822–1824.

[8]. S. Mukhopadhyay, P.K. DasPoddar, Evolution of nanoscale microstructural features in unshaped refractories by prospective spinel (MgAl2O4) gel, Interceram. 56 (2) (2007) 104–107.

[9]. S. Mukhopadhyay, P.K. DasPoddar, Evolution of nanoscale microstructural features in unshaped refractories by prospective spinel (MgAl2O4) gel, Interceram. 56 (1) (2007) 25–28;

[10]. Corrosion of Refractories, C.A. Schacht, D.A. Browson (Eds.), Refractories Handbook, Marcel Dekker Inc., New York, 2004, pp. 75.

[11]. CRC Press, LLC, Mechanochemistry,, in: H. Masuda, K. Higashitani, H.Yoshida (Eds.), 3rd edition, Powder Technology Handbook, Taylor and Francis, USA, 2006, p. 242.

[12]. K. Fujii, I. Furusato, I. Takita, Composition of spinel clinker for teeming ladle casting materials, Taikabutsu Overseas 12 (1) (1992) 4–9.

[13]. Y.C. Ko, Influence of the characteristics of spinels on the slag resistance of Al2O3–MgO and Al2O3–spinel castables, J. Am.Ceram. Soc. 83 (2000) 2333–2335.

[14]. J. Mori, M. Yoshimura, Y. Oguchi, T. Kawakami, I. Ohishi, Effect of slag composition on wear of alumina–spinel castable for steel ladle, Taikabustu Overseas 12 (1) (1992) 40–45.

[15]. H. Sarpoolaky, S. Zhang, W.E. Lee, Corrosion of high alumina and nearstoichiometric spinels in iron-containing silicate slags, J. Eur. Ceram. Soc.23 (2) (2003) 293–300.

[16]. T. Yamamura, Y. Kubota, T. Kaneshige, M. Nanba, Effect of spinel clinker composition on properties of alumina–spinel castable, Taikabutsu Overseas 13 (2) (1993) 39–45.

[17]. JIS Refractories, R2521–1995; Refractories Manual '97, The Technical Association of Refractories, Tokyo, Japan, 1997.

[18]. Y.C. Ko, Role of spinel composition in the slag resistance of Al2O3–spinel and Al2O3–MgO castables, Ceram. Int. 28 (7) (2002) 805–810.

[19]. K.M.A. Hossain, M. Lachemi, Corrosion resistance and chloride diffusivity of volcanic ash blended cement mortar, Cem. Concr. Res.34 (4) (2004) 695–702.

[20]. H.A.F. Dehwah, M. Maslehuddin, S.A. Austin, Long-term effect of sulfate ions and associated cation type on chloride-induced reinforcement corrosion in Portland cement concretes, Cem. Concr. Compos.24 (2002) 17– 25.

[21]. M. Suguwara, T. Asano, The recent developments of castable technology in Japan, in: Proceedings of the 9th UNITECR-2005, November 8–11, Orlando, FL, USA, 2005.

[22]. G. Ye, G. Oprea, T. Troczynski, Spinel bonded magnesia versus spinel bonded spinel castables, in: Proceedings of the 9th UNITECR-2005,November 8–11, Orlando, FL, USA, 2005.

[23]. V. Bhatnagar, S. Mukhopadhyay, C. Natarajan, Development of improved quality spinel castable for steel ladle bottom, in: Proceedings of the 9th UNITECR-2005, November 8–11, Orlando, FL, USA, 2005.

[24]. S. Takanaga, Y. Fujiwara, M. Hatta, Nano-Tech. refractories-3, development of MgO-rimmed MgO–C brick, in: Proceedings of the 9th UNITECR-2005, November 8–11, Orlando, FL, USA, 2005.

[25]. CemailAksel, The microstructural features of an alumina–mullite–zirconia refractory material corroded by molten glass, Ceramics International 29 (2003) 305–309

[26]. Mo´nica Popa, Masato Kakihana,Zircon formation from amorphous powder and melt in the silica-rich region of the alumina–silica–zirconia system, Journal of Non-Crystalline Solids 352 (2006) 5663–5669

[27]. Aaron J. Kessman, Karpagavalli Ramji, Zirconia sol–gel coatings on alumina–silica refractory material for improvedcorrosion resistance, Surface & Coatings Technology 204 (2009) 477–483